Absolute doubly differential cross sections for ionization of adenine by 1.0-MeV protons

Y. Iriki, Y. Kikuchi, M. Imai, and A. Itoh*

Department of Nuclear Engineering, Kyoto University, Kyoto 606-8501, Japan

(Received 21 July 2011; published 6 September 2011)

Double-differential ionization cross sections of adenine ($C_5H_5N_5$) by 1.0-MeV protons have been measured using a vapor-phase adenine target. Ejected electrons were analyzed by a 45° parallel-plate electrostatic spectrometer in an electron energy range from 1 to 1000 eV at electron emission angles from 15° to 165°. The effective target thickness of adenine was determined by a Rutherford forward scattering method and a vapor deposition method. Present data are in good agreement with recent calculations. Comparisons were made with other data on various hydrocarbon molecules. It was found that the ionization cross sections of these molecules can be scaled fairly well in terms of the total number of valence electrons.

DOI: 10.1103/PhysRevA.84.032704 PACS number(s): 34.50.Gb

I. INTRODUCTION

Ionization of atoms and molecules by energetic charged particles is the basic nature of fundamental atomic processes in matter and has been extensively studied to date [1–4]. In particular, an increasing number of experimental studies have been devoted recently to biological molecules such as amino acids and nucleic-acid-base molecules [5–7] as well as water molecules [8–11]. Theoretical investigations have also been performed extensively for nucleic-acid-base molecules [12–16] and water [17–20].

One of the primary interests in these studies is to know the spatial distributions of energy deposition in matter from various radiation species. It is known that high-energy incident particles lose their kinetic energies, forming ion tracks along their trajectories, and result in the formation of a so-called Bragg peak. A large number of secondary electrons with various energies are produced along ion tracks, especially in a Bragg peak region.

Therefore, reliable experimental data on ionization cross sections as well as stopping powers as a function of the incident energy are needed to achieve accurate evaluation of track structure and radial dose distributions. In general, ejected electrons are produced from a variety of ionization processes designated such as soft collisions, binary-encounter collisions, electron capture or loss to the continuum, and Auger processes (see,e.g., [4]). The dominant ionization among these processes arises from soft (distant) collisions which produce predominantly low-energy electrons of below 50 eV [21–23].

Ejected electrons are, on the other hand, known to play a decisive role in biological effects. Low-energy electrons may induce single- and double-strand breaks of DNA and RNA via dissociative electron attachment (DEA) reactions through the formation of shape resonances [24,25]. On the contrary, high-energy electrons like Auger electrons and δ rays can cause molecular fragmentation directly via excitation and ionization.

In this work we present absolute double-differential ionization cross sections (DDCSs) of vapor-phase adenine molecules ($C_5H_5N_5$) by 1.0-MeV proton impact. Measurements were also made for an Ar target to check the reliability of our experimental methods by comparing our cross section data with those reported by Rudd *et al.* [26]. Present results for adenine are compared with recent theoretical values reported by Lekadir *et al.* [15]. Comparison is also made with other experimental cross sections for hydrocarbon molecules [27], and the scalability of ionization cross sections among these molecules is discussed.

The paper is organized as follows. In Sec. II the experimental apparatus and procedure for deducing cross sections are described in rather detail. In Sec. III, experimental data of adenine molecules are presented and examined in terms of the classical Rutherford ionization cross sections. The scaling property of cross sections among various polyatomic molecules is discussed. Concluding remarks are given in Sec. IV.

II. EXPERIMENTAL PROCEDURE

A. Apparatus

The experiment for ionization of adenine molecules was performed at the Quantum Science and Engineering Center heavy-ion accelerator facility of Kyoto University. Figure 1 shows a schematic drawing of the experimental arrangement. A beam of 1.0-MeV protons produced by a Van de Graaff accelerator was carefully collimated to a size of about $1 \times 3\ \mathrm{mm}^2$ by a magnetic triplet quadrupole lens and charge-purified by a magnetic charge selector before entering a scattering chamber. After collision with a gas-phase target in the chamber the beam was collected by an electrically shielded Faraday cup at the end port of the beam line. A typical beam current used in the experiment was about 100 nA. A PIPS (passivated implanted planar silicon)–type solid-state detector (Canberra PD-25-12-100-AM) was also installed to measure projectile particles scattered into forward angles of 2.5° in collisions with target molecules. The inner wall of the collision chamber was covered by double permalloy magnetic shields to reduce residual or Earth magnetic fields to less than a few milligauss inside the chamber.

A molecular beam target of adenine ($C_5H_5N_5$) was produced from crystalline adenine powder of 99 at% purity contained in a 5.3-cm-long stainless-steel (SUS304) oven placed inside a copper container equipped with two cylinder-shaped heaters. Prior to measurements of secondary electrons the powder substance was heated at about 393 K for 4 h in order

*itoh@nucleng.kyoto-u.ac.jp

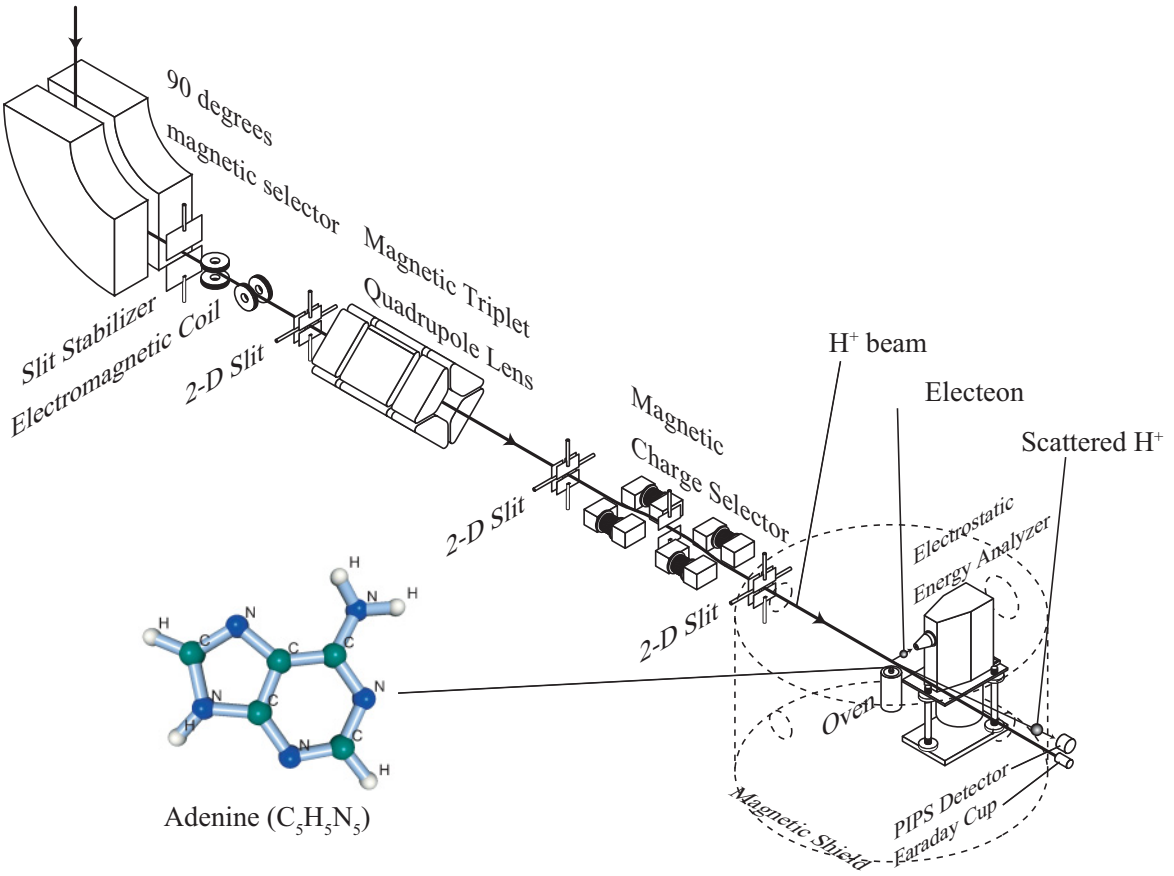

FIG. 1. (Color online) A schematic diagram of the experimental setup for ejected electron spectroscopy. The chemical structure of adenine is also shown.

to achieve a water- and impurity-free condition. Measurements were carried out at the oven temperature of 473 K. An effusive molecular beam of adenine was ejected through an outlet aperture 1 mm in diameter placed at the top of the oven and was trapped effectively by a water-cooled copper plate placed 100 mm above the proton beam line. The position of the outlet aperture was 3 mm below the beam line. The spot size of the molecular vapor target at the position of the beam line was measured prior to the experiment by a vapor deposition method. The observed vapor spot deposited on a cold copper plate placed at this height was about 3 mm in diameter.

A base pressure of the collision chamber, evacuated by two turbomolecular pumps with pumping speeds of 600 and 300 L/s, was kept below 2×10^{-7} Torr during the experiment. The background contribution from residual gases to cross-section data was found to be negligibly small.

Ejected electrons were analyzed by a 45° parallel-plate electrostatic spectrometer [28,29] mounted on a turntable controlled by a pulse motor. Electrons were detected by a channel electron multiplier (CEM). Measurements were carried out for an electron energy range from 1 to 1 keV and an emission angle range from 15° to 165° at 15° intervals with respect to the incident H^+ beam direction. A gap distance between the upper and the lower electrode plates of the spectrometer was 15 mm. The width and length of the electron entrance and exit slits located at a distance of 49.5 mm apart from each other were 2 and 10 mm, respectively. The space between the plates was surrounded by five rectangular electrodes connected to resistors to ensure a uniform electric field between the two plates. The energy resolution $\Delta\epsilon/\epsilon$ was 8% at FWHM. In order to collect efficiently low-energy electrons of a few electron volts, a positive bias of 40 V was placed on the lower electrode plate.

The experiment was conducted with a computer-controlled data acquisition system. The analyzing voltage placed on the upper electrode of the spectrometer was supplied by a high-precision power supply (Kepco Inc.; BOP1000M). The channel advance was made automatically after collecting a constant amount of proton beam current with the Faraday cup. All experimental parameters such as electron signal counts, analyzing voltages measured by a digital multimeter, pulse heights of forwardly scattered protons measured by the PIPS detector, and pressures of the collision chamber were stored digitally in each channel.

B. Differential cross sections

DDCSs for the ejection of electrons with energy ϵ and emission angle θ were obtained from the equation

$$\sigma(\epsilon,\theta) \equiv \frac{d^2\sigma}{d\epsilon d\omega} = \frac{y(\epsilon,\theta) - y_b(\epsilon,\theta)}{I_P \eta \Delta\epsilon \Delta\omega N_T \ell_v}, \quad (1)$$

where $y(\epsilon,\theta)$and $y_b(\epsilon,\theta)$ are, respectively, the number of electrons detected with and without a vapor target, I_P is

the number of incident protons, $\Delta\epsilon = 0.08\epsilon is$ the energy spread at ϵ, $\Delta\omega$ is the solid angle of the spectrometer, and $\eta = 51.8\%$ is the total detection efficiency given by the product of the spectrometer transmission, the open-area ratio of four meshes, and the CEM efficiency. N_T is the number density of the vapor target and $\ell_v (\simeq 3$ mm) the length of the target seen by the spectrometer. It should be noted here that ℓ_v is smaller than the length of the proton beam seen by the spectrometer ($\ell_0 = 6$ mm) at $\theta = 90^\circ$. Thus, the target length is the same irrespective of θ in the present work. The product $N_T \ell_v$ gives the effective target thickness and was determined simultaneously by Rutherford forward scattering as described in Sec. II C (below).

Single-differential cross sections (SDCSs) were obtained by integrating the DDCS over the solid angle as

$$\sigma(\epsilon) \equiv \frac{d\sigma}{d\epsilon} = 2\pi \int_0^\pi \sigma(\epsilon,\theta) \sin\theta d\theta. \quad (2)$$

Data extrapolated to $\theta = 0$ and π were used in the integration. The total ionization cross sections (TICSs) were obtained from

$$\sigma_t = \int_{\epsilon_1}^{\epsilon_2} \sigma(\epsilon) d\epsilon, \quad (3)$$

with $\epsilon_1 = 1$ eV and $\epsilon_2 = 1000$ eV.

C. Measurements of the effective target thickness

The effective target thickness $N_T \ell_v$ was determined by the use of Rutherford forward scattering of projectile ions into a 2.5° direction. A circular aperture 2 mm in diameter was placed in front of the PIPS detector. As the vapor target in the beam line was restricted to a spot about 3 mm in diameter, the acceptance angle of the detector for scattered particles was limited to $2.5 \pm 0.1^\circ$.

The effective target thickness was obtained from the following equation,

$$Y(\theta_p) - Y_b(\theta_p) = I_P N_T \ell_v \sigma_R(\theta_p) \Delta\Omega_p, \quad (4)$$

where $Y(\theta_p)$ and $Y_b(\theta_p)$ are the scattering yields measured with and without a vapor target at the scattering angle $\theta_p (=2.5^o)$, $\sigma_R(\theta_p)$ is the Rutherford scattering cross section per unit solid angle and $\Delta\Omega_p$ is the solid angle of the PIPS detector. It is noted that $\sigma_R(\theta_p)$ is the sum of scattering cross sections of constituent atoms of adenine. The scattering cross section used in this work is described in the Appendix.

D. Measurements for Ar

As a system check of our experimental apparatus, we carried out measurements for an Ar target for which previous experimental data are available in the literature [26]. An argon gas was introduced into the chamber through a fine-needle valve welded to a flange of the scattering chamber. In this measurement, the pressure distribution along the proton beam line inside the chamber was practically homogeneous. Ejected electron measurements were made at a target pressure of about 5×10^{-5} Torr measured by a calibrated ionization gauge. The number density N_T of Ar atoms was calculated by applying the ideal-gas model at room temperature.

It is noted that, in this case, the effective target length seen by the spectrometer is given by $\ell_0 / \sin\theta$ instead of ℓ_v in Eq. (1).

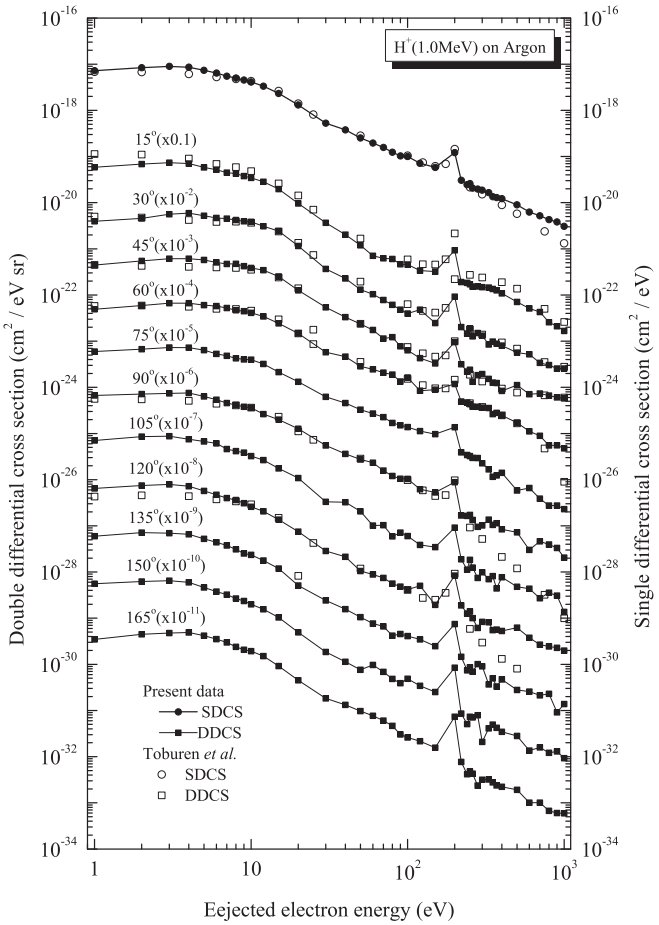

FIG. 2. Double-differential cross sections (DDCS) for ejection of electrons by 1.0-MeV protons in Ar. The uppermost energy distribution is the single-differential cross section (SDCS) obtained by integrating the DDCSs, which are plotted by multiplying scaling factors as shown in parentheses. Data from Ref. [26] are shown by open symbols for comparison.

Absolute DDCSs measured for Ar by 1.0 MeV protons are shown by filled squares in Fig. 2. Data at different angles are scaled by multiplying appropriate scaling factors, shown in parentheses, to avoid confusion. The uppermost energy spectrum, shown by filled circles, presents $\sigma(\epsilon)$ obtained from Eq. (2). Comparison with other data tabulated by Rudd *et al.* [26] shows that the present data are in good agreement with them.

III. RESULTS AND DISCUSSION

A. Cross sections for adenine

DDCSs for electron emission from adenine impacted by 1.0-MeV protons are presented in Fig. 3 and in the Supplemental Material [30]. Data were taken for electron energies from 1 to 1000 eV at 11 emission angles between 15° and 165°. SDCSs $\sigma(\epsilon)$ are also shown as the uppermost energy spectrum in Fig. 3.

One can see that all the DDCS spectra exhibit broad humps below 10 eV, which is largely different from the case of an Ar target. This hump structure was confirmed by repeating measurements under various conditions of heater currents and

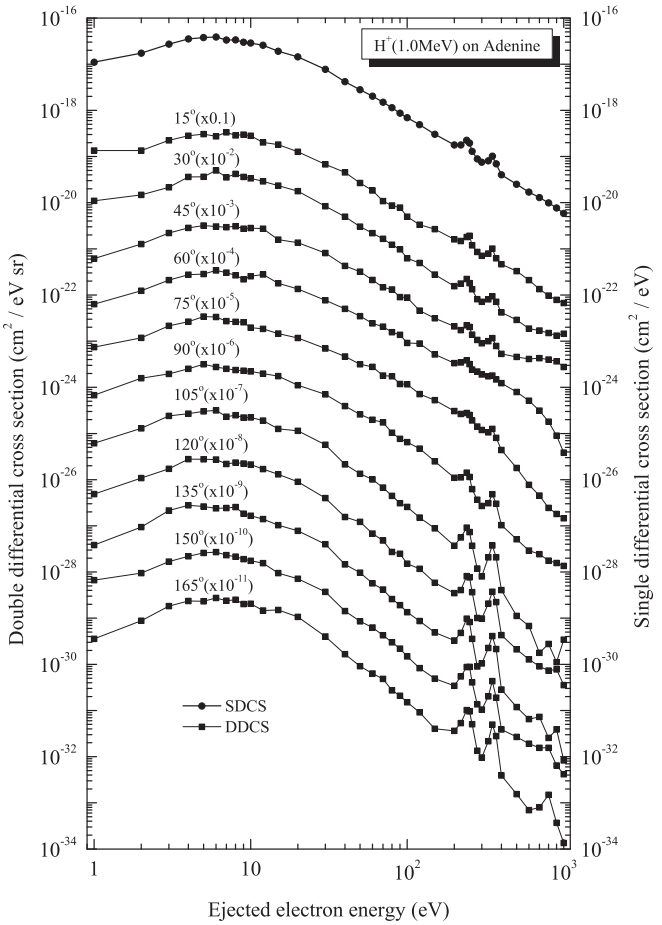

FIG. 3. Double-differential cross sections (DDCSs) for ejection of electrons by 1.0-MeV protons in adenine. The uppermost energy distribution is the single-differential cross section (SDCS) obtained by integrating the DDCSs, which are plotted by multiplying scaling factors as shown in parentheses. Two peaks, at approximately 250 and 400 eV, are the *K-LL* Auger electrons from carbon and nitrogen, respectively.

heights of the oven. The measurement was also made under a power-off condition of the oven heaters after reaching 473 K. Nevertheless, the humps were always reproduced fairly well, indicating no magnetic field effects from the oven. From the fact that the hump structure does not change at different gas densities measured at different oven temperatures, loss of low-energy electrons ($\epsilon < 10$ eV) due to elastic scattering by adenine molecules may be ruled out, although somewhat large scattering cross sections of low-energy electrons by pyrimidine bases of DNA are reported [31]. As the second feature, we found that low-energy electrons with $\epsilon \leqslant 30$ eV are ejected nearly isotropically. Two peaks, located at about 250 and 400 eV, are *K-LL* Auger electrons emitted from carbon and nitrogen, respectively. The classical binary encounter peaks at $\epsilon(\mathrm{eV}) = 4T\cos^2\theta$ appear at emission angles $\theta \leqslant 75^\circ$, with $T = 544$ eV the energy of electron with the incident proton velocity.

Since no other experimental results are available for adenine, we examined the present results in the following way. As described in experimental work [32] and in the review article by Rudd [2], it may be possible to check the

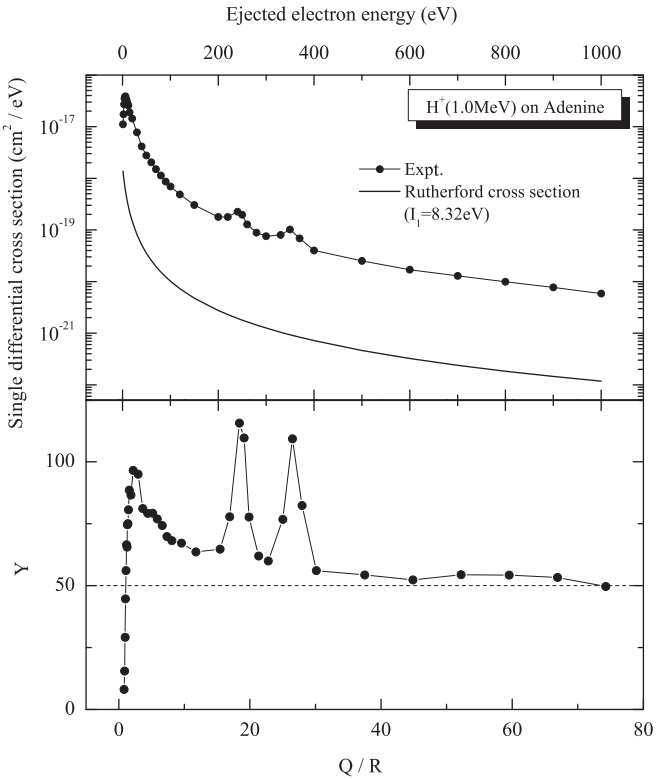

FIG. 4. Top: A comparison of our SDCS for adenine with the Rutherford cross section calculated with $I_1 = 8.32$ eV. Bottom: Platzman plot of the SDCS obtained as the ratio of $\sigma(\epsilon)$ to the Rutherford cross section. The abscissa Q/R is the energy transfer $Q = \epsilon + I$ divided by the Rydberg energy R. The horizontal dotted line shows the total number of valence electrons of adenine.

reliability of our measured cross sections by comparing them with Rutherford cross sections between an incident particle and a bound electron in the target molecule. The ratio Y of the experimental SDCS $\sigma(\epsilon)$ to the Rutherford cross section per electron is given by

$$Y = \frac{T}{4\pi a_0^2}\left(\frac{Q}{R}\right)^2 \sigma(\epsilon), \tag{5}$$

where $Q = \epsilon + I$ stands for the energy transfer to an electron with binding energy I, a_0 the Bohr radius, and $R = 13.6$ eV the Rydberg energy. Plotting the ratio Y as a function of Q/R is called a Platzman plot [2,33], and the value of Y for sufficiently high electron energies is supposed to approach the effective number of electrons in the target which participate in the ionization event of interest. Figure 4 shows the Platzman plot of our SDCS for the ionization of adenine by 1.0-MeV protons. Here we used $I_1 = 8.32$ eV as the first ionization potential of adenine [15]. Similarly to the interpretation by Rudd [2] made for Ar ionization by protons, it is possible to state that the lower part, below $Q/R < 20$, represents the contribution from the dipole term. Two peaks, at $Q/R = 18$–26, arise from *K-LL* Auger electrons. As the dipole interaction term diminishes with increasing Q/R, the ratio Y approaches the effective number of target electrons in the participating shells [2]. Actually, the present result is close to 50, the number of valence

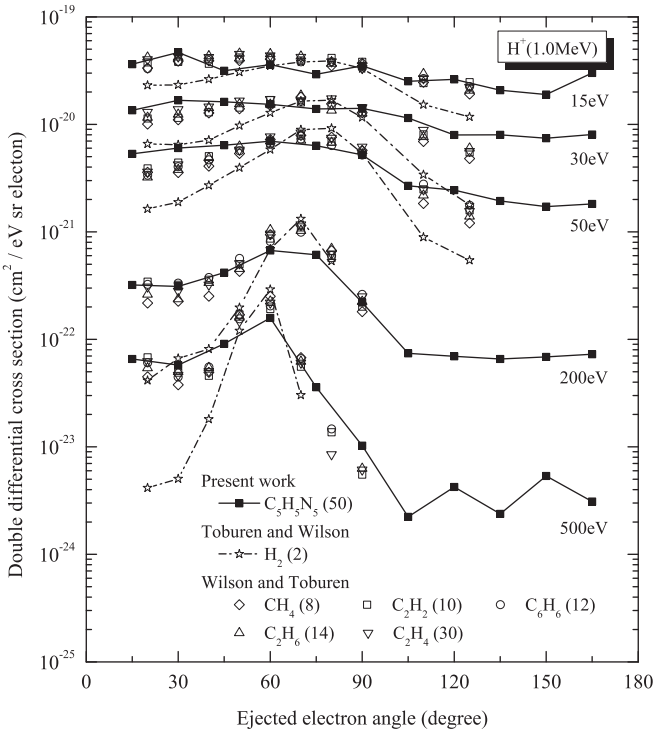

FIG. 5. Angular distribution of ejected electrons for electron energies of $\epsilon = 15$, 30, 50, 200, and 500 eV. Data are plotted by dividing the DDCS by n_v. Data for other molecules are taken from [36] for H_2 and [27] for five hydrocarbon molecules. Numbers in parentheses represents the n_v of molecules.

electrons of adenine, shown by the horizontal dotted line in Fig. 4.

B. Scaling properties of differential cross sections

Wilson and Toburen investigated the scalability of the DDCS and SDCS for various hydrocarbon molecules [27,34,35]. They found an excellent scalability of these cross sections in terms of the number of valence electrons n_v in molecules. Here, tightly bound 1*s*-shell electrons of atoms except for hydrogen are excluded. This scalability is reasonable because ionization of a molecule by a fast charged particle is dominated by weakly bound outer-shell electrons. The DDCSs of our adenine data divided by $n_v = 50$ are shown in Fig. 5 as a function of the electron emission angle θ at electron energies $\epsilon = 15, 30, 50, 200$, and 500 eV, respectively. Figure 5 also shows the $\sigma(\epsilon,\theta)/n_v$ of other hydrocarbon molecules of methane (CH_4,;$n_v = 8$), acetylene (C_2H_2; $n_v = 10$), ethylene (C_2H_4; $n_v = 12$), ethane (C_2H_6; $n_v = 14$), and benzene (C_6H_6; $n_v = 30$) measured by Wilson and Toburen [27]. Although the number of valence electrons and the chemical structures of individual molecules are considerably different from one another, overall angular distributions of all these molecules are in relatively good agreement at all the emission angles. Note that the data on H_2 deviate significantly from those for other polyatomic molecules.

A fairly good scalability is also seen for SDCSs as a function of the electron energy as shown in Fig. 6. It shows clearly that the scalability holds fairly well for an electron energy $\epsilon > 10$ eV. The binding energies of valence electrons are well

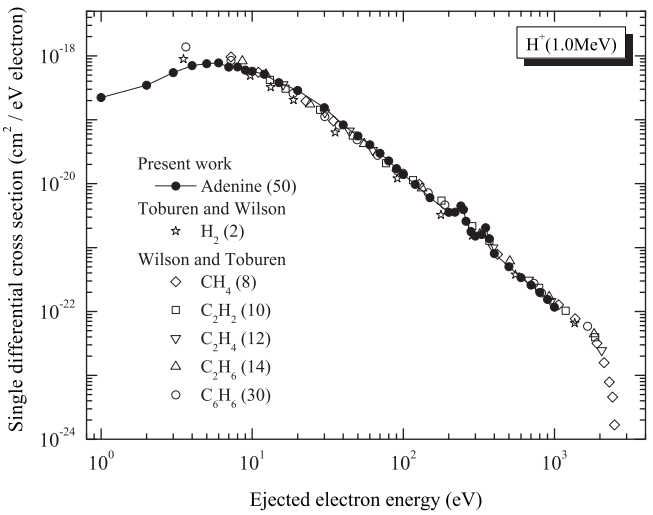

FIG. 6. SDCSs divided by n_v for adenine and other various hydrocarbon molecules. Data are taken from [36] for H_2 and [27] for hydrocarbons.

confined below 40 eV irrespective of the molecules [2,15]. This fact may be the main reason why the scalability holds so well among these molecules.

C. Total ionization cross section

Figure 7 shows TICSs σ_t of various polyatomic molecules obtained for 1.0-MeV proton impacts [1,27,35], where all the data are plotted as a function of n_v. One can see that all these cross sections lie on a straight line fairly well. Applying the least-squares fit to these data gives a relationship of

$$\sigma_t[\mathrm{cm}^2] = 0.172 n_v 10^{-16}. \quad (6)$$

Here, the coefficient 0.172×10^{-16} [cm^2] should be equivalent to the TICS of a single-valence electron. It is pointed out that

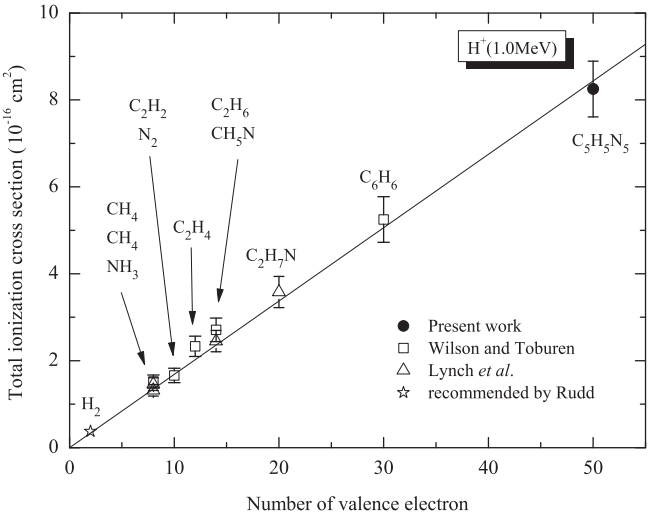

FIG. 7. Total ionization cross sections versus n_v of adenine and various molecules obtained for 1.0-Mev proton impact. Data are taken from [1] for H_2 and from [27] and [35] for other molecules. All data points are well on the straight line of $0.172 n_v \times 10^{-16}$ cm^2.

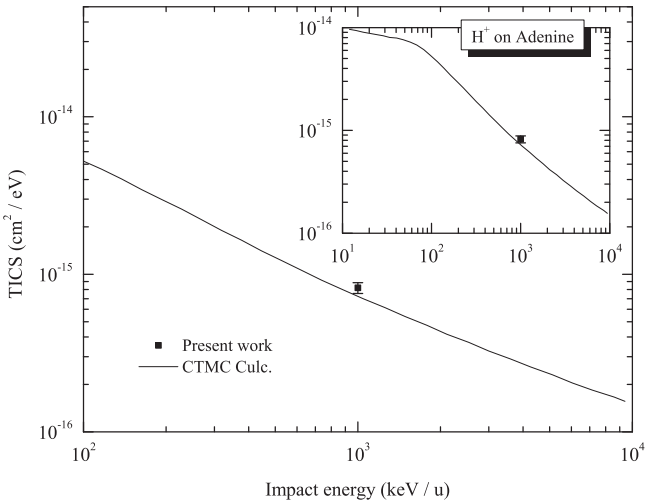

FIG. 8. Present total ionization cross section of adenine is compared with CTMC calculations [15]. The abscissa is the incident proton energy (keV/U).

the classical Rutherford TICS, approximated by $4\pi a_0^2 R^2/TI$, gives the same value if we use $I \simeq 7.0$ eV. The present value multiplied by 2 also compares the recommended TICS of 0.375×10^{-16} for H_2 given by Rudd [1]. Note that their recommended TICS for atomic hydrogen is 0.192×10^{-16}, which is about 10% larger than our value.

Finally, the present TICS is compared in Fig. 8 with recent theoretical results obtained by classical trajectory Monte Carlo (CTMC) calculations [15]. The present result is about 10% larger than their value at 1.0 MeV. This may be attributed to the large contribution of low-energy electrons due to the dipole interaction, which is not considered in their CTMC calculations.

IV. CONCLUSION

Ionization cross sections of adenine by the impact of 1.0-MeV protons have been measured by ejected electron spectroscopy. To obtain accurate cross-section data, care was taken to reduce uncertainties as much as possible arising from various sources such as the Earth's magnetic field in the chamber, stray magnetic fields induced by heater currents of the oven, and the effective target length of effusive adenine molecules. In particular, the effective target length was determined by a vapor-deposition method and by the Rutherford forward-scattering method. As a check of the reliability of our experimental apparatus, we measured DDCSs for an Ar target. Our data were found to be consistent with previous data obtained by Rudd *et al.* [2].

The Platzman plot of experimental cross section $\sigma(\epsilon)$ vs Q/R reasonably reveals the total number of target electrons contributing to the ionization cross sections. Furthermore, the cross sections of various polyatomic molecules including adenine are found to be scaled fairly well by using n_v, the number of outer-shell electrons of target molecules. Namely, the cross sections divided by n_v are nearly equivalent to those of various hydrocarbon molecules, despite different values of n_v and chemical structures of individual molecules. The TICS is well scaled by $\sigma_t = 0.172 n_v \times 10^{-16}$ cm^2 for these molecules. This is due to the fact the binding energies of outer shells are not greatly different among these polyatomic molecules and the contribution from inner-shell ionization can be practically ignored. Extension of measurements to different incident proton energies is needed to examine theoretical calculations.

ACKNOWLEDGMENTS

This work was supported by Grant-in-Aid for Scientific Research (B), No. 16360474, from the Japan Society for the Promotion of Science. We acknowledge Mr. K. Doi, Mr. M. Naitoh, Mr. K. Yoshida, Mr. K. Norizawa, Dr. H. Shibata, and Dr. H. Tsuchida for their technical support during experiments.

APPENDIX A:RUTHERFORD SCATTERING CROSS SECTION

As for the forward-scattering cross section of incident protons, we used the modified Rutherford cross section [37], given in the laboratory frame by

$$\sigma_R(\theta, z_2) = F(z_2)\left(\frac{z_1 z_2}{2E_1}\right)^2 \times \frac{\left(\cos\theta + \sqrt{1-\gamma^2\sin^2\theta}\right)^2}{\sin^4\theta\sqrt{1-\gamma^2\sin^2\theta}}. \quad \text{(A1)}$$

Here, $\sigma_R(\theta, z_2)$ is the scattering cross section per unit solid angle for an incident particle with nuclear charge z_1 and energy E_1 by a target atom with nuclear charge z_2, $\gamma = m_1/m_2$ is the mass ratio between the two particles, and θ is the scattering angle in the laboratory frame. $F(z_2)$ is the correction factor arising from the screening of z_2 by target electrons and, for $\theta < 90^o$, is expressed as

$$F(z_2) = \left(1 + \frac{V_1}{2E_{\rm cm}}\right)^2 \times \left[1 + \frac{V_1}{E_{\rm cm}} + \left(\frac{V_1}{2E_{\rm cm}\sin(\Theta/2)}\right)^2\right]^{-2}, \quad \text{(A2)}$$

where $E_{\rm cm} = E_1/(1+\gamma)$ and Θ are the incident energy and the scattering angle in the center-of-mass system and V_1 denotes the increase in the kinetic energy of the projectile due to the screening effect,

$$V_1[\text{keV}] = 0.04873 z_1 z_2 \left({z_1}^{2/3} + {z_2}^{2/3}\right)^{1/2}. \quad \text{(A3)}$$

Note that we used the following simple relationship between θ and Θ obtained for pure Rutherford scattering between two bare ions:

$$\cos\Theta = -\gamma\sin^2\theta + \cos\theta\sqrt{1-\gamma^2\sin^2\theta}. \quad \text{(A4)}$$

The total Rutherford cross section per adenine molecule is the sum of cross sections for constituent atoms of H, C, and N in the molecule, as obtained by

$$\sigma_R(\theta) = \sum_{z_{2i}} N(z_{2i}) F(z_{2i}) \sigma_R(\theta, z_{2i}), \quad \text{(A5)}$$

where $N(z_{2i})$ is the number of each atom in the molecule.

[1] M. E. Rudd, Y.-K. Kim, D. H. Madison, and J. W. Gallagher, Rev. Mod. Phys. **57**, 965 (1985).
[2] M. E. Rudd, Y.-K. Kim, D. H. Madison, and T. J. Gay, Rev. Mod. Phys. **64**, 441 (1992).
[3] M. E. Rudd, Y.-K. Kim, T. Märk, J. Schou, N. Stolterfoht, L. Toburen, H. Bichsel, R. Dubios, H. Wyckoff, W. Ney *et al.*, *Secondary Electron Spectra from Charged Particle Interactions. ICRU, Report 55* (International Comission on Radiation Units and Measurements, Bethesda, MD, 1995).
[4] N. Stolterfoht, R. D. DuBois, and R. D. Rivaola, *Electron Emission in Heavy Ion Atom Collision* (Springer, Berlin, 1997).
[5] P. Moretto-Capelle and A. Le Padellec, Phys. Rev. A **74**, 62705 (2006).
[6] J. Tabet, S. Eden, S. Feil, H. Abdoul-Carime, B. Farizon, M. Farizon, S. Ouaskit, and T. D. Märk, Phys. Rev. A **81**, 012711 (2010).
[7] J. Tabet, S. Eden, S. Feil, H. Abdoul-Carime, B. Farizon, M. Farizon, S. Ouaskit, and T. D. Märk, Phys. Rev. A **82**, 022703 (2010).
[8] D. Ohsawa, H. Kawauchi, M. Hirabayashi, Y. Okada, T. Honma, A. Higashi, S. Amano, Y. Hashimoto, F. Soga, and Y. Sato, Nucl. Instrum. Methods Phys. Res. Sec. B **227**, 431 (2004).
[9] D. Ohsawa, Y. Sato, Y. Okada, V. P. Shevelko, and F. Soga, Phys. Rev. A **72**, 062710 (2005).
[10] D. Ohsawa, Y. Sato, Y. Okada, V. P. Shevelko, and F. Soga, Phys. Lett. A **342**, 168 (2005).
[11] F. Gobet, S. Eden, B. Coupier, J. Tabet, B. Farizon, M. Farizon, M. J. Gaillard, M. Carré, S. Ouaskit, T. D. Märk *et al.*, Phys. Rev. A **70**, 062716 (2004).
[12] H. Lekadir, I. Abbas, C. Champion, and J. Hanssen, Nucl. Instrum. Methods Phys. Res. Sec. B **267**, 1011 (2009).
[13] I. Abbas, C. Champion, B. Zarour, B. Lasri, and J. Hanssen, Phys. Med. Biol. **53**, N41 (2008).
[14] C. Dal Cappello, P. A. Hervieux, I. Charpentier, and F. Ruiz-Lopez, Phys. Rev. A **78**, 042702 (2008).
[15] H. Lekadir, I. Abbas, C. Champion, O. Fojón, R. D. Rivarola, and J. Hanssen, Phys. Rev. A **79**, 062710 (2009).
[16] C. Champion, H. Lekadir, M. E. Galassi, O. Fojón, R. Rivarola, and J. Hanssen, Phys. Med. Biol. **55**, 6053 (2010).
[17] C. Champion, O. Boudrioua, C. D. Cappello, Y. Sato, and D. Ohsawa, Phys. Rev. A **75**, 32724 (2007).
[18] O. Boudrioua, C. Champion, C. D. Cappello, and Y. V. Popov, Phys. Rev. A **75**, 22720 (2007).
[19] C. Dal Cappello, C. Champion, O. Boudrioua, H. Lekadir, S. Y., and D. Ohsawa, Nucl. Instrum. Methods Phys. Res. Sec. B **267**, 781 (2009).
[20] C. Champion and C. Dal Cappello, Nucl. Instrum. Methods Phys. Res. Sec. B **267**, 881 (2009).
[21] S. Uehara, H. Nikjoo, and D. T. Goodhead, Radiat. Res. **152**, 202 (1999).
[22] J. A. LaVerne and S. M. Pimblott, Radiat. Res. **141**, 208 (1995).
[23] L. Sanche, Eur. Phys. J. D **35**, 367 (2005).
[24] B. Boudaïffa, P. Cloutier, D. Hunting, M. A. Huels, and L. Sanche, Science **287**, 1658 (2000).
[25] S. Gohlke, A. Rosa, E. Illenberger, F. Brüning, and M. A. Huels, J. Chem. Phys. **116**, 10164 (2002).
[26] M. E. Rudd, L. H. Toburen, and N. Stolterfoht, At. Data Nucl. Data Tables **23**, 405 (1979).
[27] W. E. Wilson and L. H. Toburen, Phys. Rev. A **11**, 1303 (1975).
[28] G. A. Harrower, Rev. Sci. Instrum. **26**, 850 (1955).
[29] N. Stolterfoht, Z. Physik **248**, 81 (1971).
[30] See Supplemental Material at http://link.aps.org/supplemental/10.1103/PhysRevA.84.032704 for numeric data on double-differential cross sections.
[31] V. M. C. Winstead and S. Sanchez, J. Chem. Phys. **127**, 085105 (2007).
[32] L. H. Toburen and W. E. Wilson, Phys. Rev. A **19**, 2214 (1979).
[33] W. F. Miller and R. L. Platzman, Proc. Phys. Soc. London Sec. A **70**, 299 (1957).
[34] L. H. Toburen and W. E. Wilson, J. Chem. Phys. **66**, 5202 (1977).
[35] D. J. Lynch, L. H. Toburen, and W. E. Wilson, J. Chem. Phys. **64**, 2616 (1976).
[36] L. H. Toburen and W. E. Wilson, Phys. Rev. A **5**, 247 (1972).
[37] H. H. Andersen, F. Besenbacher, P. Loftager, and W. Möller, Phys. Rev. A **21**, 1891 (1980).